Front. Struct. Civ. Eng. 2020, 14(3): 706–721
https://doi.org/10.1007/s11709-020-0612-9

RESEARCH ARTICLE

Semi-active fuzzy control of Lali Cable-Stayed Bridge using MR dampers under seismic excitation

Sajad JAVADINASAB HORMOZABAD, Amir K. GHORBANI-TANHA*

School of Civil Engineering, College of Engineering, University of Tehran, Tehran 11155-4563, Iran
**Corresponding author. E-mail: ghtanha@ut.ac.ir*

ABSTRACT Seismic control of cable-stayed bridges is of paramount importance due to their complex dynamic behavior, high flexibility, and low structural damping. In the present study, several semi-active Fuzzy Control Algorithms (FCAs) for vibration mitigation of Lali Cable-Stayed Bridge are devised. To demonstrate the efficiency of the algorithms, a comprehensive nonlinear 3-D model of the bridge is created using OpenSees. An efficient method for connecting MATLAB and OpenSees is devised for applying FCAs to the structural model of the bridge. Two innovative fuzzy rule-bases are introduced. A total of six different fuzzy rule-bases are utilized. The efficiency of the FCAs is evaluated in a comparative manner. The performance of fuzzy control systems is also compared with a sky-hook and a passive-on system. Moreover, the sensitivity of efficiency of control systems to the peak ground acceleration is evaluated qualitatively. In addition, the effect of time lag is also investigated. This study thoroughly examines the efficiency of the FCAs in different aspects. Therefore, the results can be regarded as a general guide to design semi-active fuzzy control systems for vibration mitigation of cable-stayed bridges.

KEYWORDS semi-active control, Fuzzy Control Algorithm, cable-stayed bridge, MR damper, Lali Bridge

1 Introduction

Among different types of bridges, cable-stayed bridge is prominent for its effective structural behavior, reasonable cost, and attractive appearance [1,2]. However, the dynamic behavior of cable-stayed bridges includes some remarkable complexities due to deck pre-stressing [3], combined horizontal, vertical and torsional deflections [4], or coupled bending and torsional mode shapes [5]. In addition, high flexibility and low structural damping of these bridges make them highly vulnerable to dynamic environmental loadings such as wind, earthquake, and traffic loads [6]. Accordingly, utilizing structural control technologies in order to reduce the dynamic response and provide safety and serviceability against dynamic loads seems to be crucial for cable-stayed bridges [7–10].

With the length of 460 m, Lali Bridge is regarded as the longest cable-stayed bridge in Iran. It is located in Khouzestan Province and crosses the Karoun River. Because of the great importance of this bridge and the earthquake-prone area in which it is located, its seismic behavior is by far an essential issue which should be investigated precisely [11]. Therefore, it is necessary to use a powerful finite element software to achieve a comprehensive model of the Lali Bridge. The model must be capable of simulating the complex nonlinear behavior of different types of elements, especially the reinforced concrete (RC) and pre-stressed cable elements. Vibration control of such important structure is considered as a beneficial and economical method in order to reduce hazard probability.

The most important drawback of active control systems is their remarkable energy consumption. On the other hand, some studies have shown that semi-active systems can almost exhibit the performance of active systems without any need for so remarkable energy supplies [12]. Therefore, the application of semi-active or adaptive systems for reducing the wind- and earthquake-induced vibrations has been thoroughly investigated in some studies [13–17].

In past decades, numerous hazardous events in cable-stayed bridges caused by sever earthquakes evoked a

Article history: Received Dec 18, 2018; Accepted May 16, 2019

serious need for defining a benchmark problem. Hence, the benchmark control problem for cable-stayed bridges was developed by Dyke et al. [18]. Afterwards, different control methods were proposed and evaluated for mitigating the earthquake-induced vibrations of the benchmark bridge [19–21].

Dyke et al. [22] proposed a clipped-optimal algorithm controlling the command voltage of MR dampers in seismically excited structures. Afterwards, the application of clipped-optimal algorithm in feedback control systems with MR dampers was also investigated by Jansen and Dyke [23], Yi et al. [24], and Ramallo et al. [25]. Another strategy intended to control the damping force of MR dampers was introduced by Xu and Li [26]. They proposed a multi-step predictive control algorithm implemented numerically on a 11-story building structure and observed that the system shows remarkable efficiency in vibration reduction as well as high stability against time delay.

Jung et al. [27] proposed several patterns to describe the mechanical behavior of MR fluid dampers. Based on experimental data, they finally suggested three mechanical models for MR dampers: Bingham, Bouc-Wen, and modified Bouc-Wen model.

Fuzzy logic controllers are also effective alternatives for semi-active control of cable-stayed bridges because they can be effectively applied to multivariable and nonlinear systems. Moreover, a fuzzy system uses linguistic variables and therefore is easy to understand and does not necessarily require crisp data. Symans and Kelly [28] developed eight different fuzzy rule-bases for controlling the bridge structures and introduced three of them typically producing the most significant response reductions. Park et al. [29] proposed a fuzzy supervisory system for vibration control of cable-stayed bridges. The system is comprised of a fuzzy controller along with several sub-controllers. Ok et al. [30] investigated the application of MR dampers for promoting the seismic performance of cable-stayed bridges. In their study, the command voltage is determined using a fuzzy controller. They applied the control system to the benchmark bridge and demonstrated that the semi-active fuzzy controller can remarkably improve the performance of MR dampers.

MR dampers are adaptive control devices which can produce controllable damping force using MR fluids. They can operate effectively for a wide range of excitation frequency and provide relatively large control forces. They require small power supplies and exhibit remarkably robust and reliable performance. Several studies have shown that in specific conditions the performance of an MR damper can be almost equal to that of an active system [22,23,25,31,32].

Preliminary studies have been carried out to investigate the seismic behavior and passive vibration control of Lali Cable-Stayed Bridge [11]. In present study, a comprehensive nonlinear 3-D model of the Lali Bridge is created using OpenSees. Seismic response of the bridge is investigated using adequate earthquake excitation records. Some semi-active fuzzy control systems comprised of MR fluid dampers are utilized in order to mitigate the vibrations of the bridge subjected to different excitation records. Some evaluation criteria describing the performance of the control algorithms are considered. Two new fuzzy rule-bases are utilized, along with four rule-bases suggested by other researches. The efficiency of six different Fuzzy Control Algorithms (FCAs) are compared to each other and also to their sky-hook and passive counterparts. The sensitivity of efficiency of control systems to the Peak Ground Acceleration (PGA) is evaluated qualitatively. Finally, the effect of time lag is included to measure the consequential drop in the performance. In the past studies, because of the difficulties with simulating nonlinear behavior of cable-stayed bridges and updating the stiffness matrices in each step of analysis, “linear models” are used in order to employ semi-active algorithms for reducing the vibrations of cable-stayed bridges. In this study, unlike most of the past research efforts, semi-active control algorithms are applied to the “nonlinear” model of the cable-stayed bridge using an efficient method for connecting MATLAB and OpenSees.

2 Structural model of the Lali Cable-Stayed Bridge

2.1 Introduction to the Lali Cable-Stayed Bridge

The Lali Bridge, which is known as the longest bridge in Iran, passes across the reservoir formed by the new Gotvand-Olya Dam. With a total length of 460 m the bridge is comprised of three main spans: a central span of 256 m and two side spans of 102 m. The deck includes two lanes of a total width of 13.5 m. Before 2011, the elevation of river surface was roughly about 104 m, i.e., 15 m beneath the deck, but after construction of the dam it increased up to 230 m. The Karun River is regarded as the most important power producing waterway in the country thanks to its outstanding discharge.

The Lali Bridge includes two main piers with an approximate height of 145 m. The piers are made up of five different cross sections. A caisson foundation is constructed beneath each pier. The deck of the caissons is 16 by 32 m with a thickness of 5 m. The caissons are of 10 m diameter and have a depth of 20 m in the rock. The deck is connected to the piers using a total of 80 stayed cables. The diameter of the cables varies between 4.8 and 7.2 cm. Some general information about the Lali Bridge are presented in Figs. 1 and 2.

2.2 Nonlinear finite element model of the bridge

To simulate the seismic behavior of the bridge, a comprehensive structural model is created in OpenSees

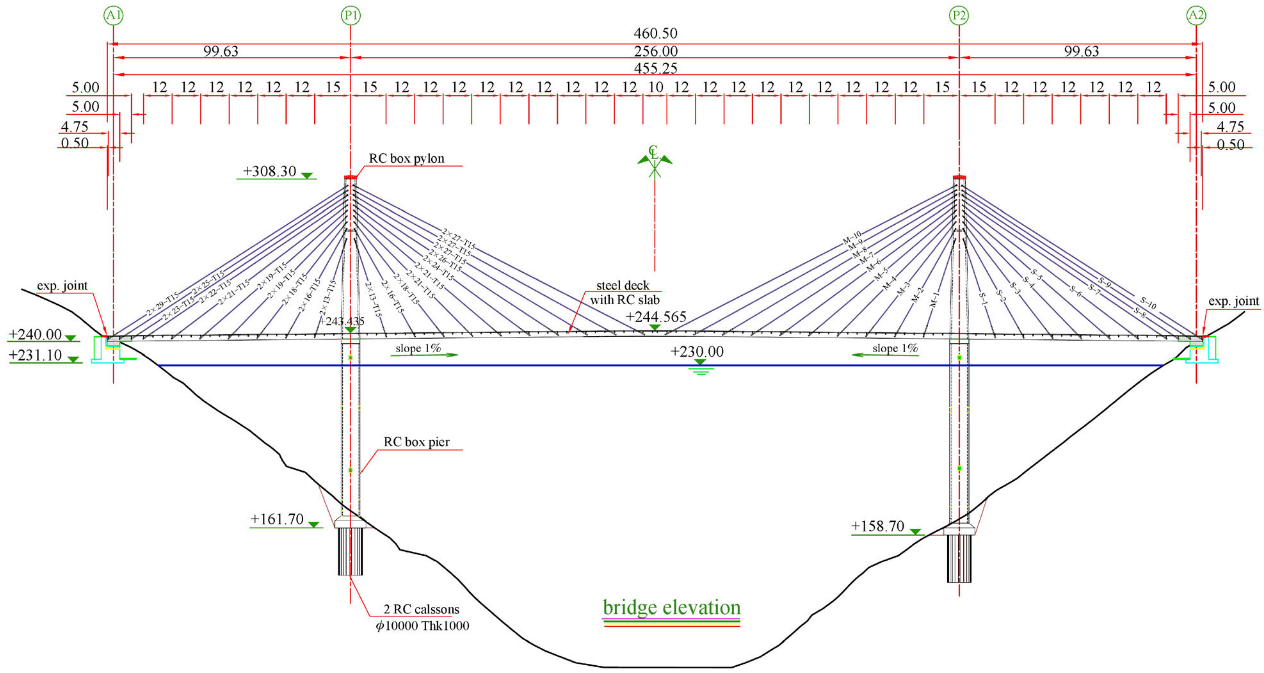

Fig. 1 Overall layout of the Lali Bridge (dimensions in m).

based on an existing SAP2000 model provided by the design company (Fig. 3(a)). In OpenSees model, the piers, deck girders, and secondary beams of the deck are created using beam-column elements and fiber sections. Simulating the behavior of pre-stressed stay cables has its complexities and is thoroughly investigated by Salari et al. [33]. Herein, stay cables are created using truss elements and ElasticPPGap material. Mechanical behavior of this material is shown in Fig. 3(b). The material only acts in tension and the amount of the gap is determined based on the desired pre-stress force. In other words, the point where the graph intersects the vertical axis, determines the amount of initial pre-stress force available in each cable.

Each end of the deck is connected to abutment using two horizontal and two vertical spring elements. The horizontal-transversal deformation (along Y axis) of the deck is fully restricted. The stiffness of spring elements in horizontal-longitudinal and vertical direction (along X and Z axis) is 1280 and 1350280 ton/m, respectively. Each pier is connected to the ground at seven points. At each point, three spring elements in X, Y, and Z direction are implemented. The stiffness of spring elements in X and Z direction is 588240 ton/m and the corresponding value in Y direction is 625000 ton/m. Complementary information about the finite element model of the Lali Bridge as well as the mechanical characteristics of the MR dampers implemented on the bridge are presented in Tables 1 and 2. The soil profile type is reported to be S_b (Rock) according to UBC [34], and therefore, the soil-structure interaction can be ignored.

The first six mode shapes obtained from SAP2000 are demonstrated in Fig. 4. The first mode shape is mainly related to the transversal deflection of the deck in horizontal plane. In this mode shape, the piers move laterally in the same direction. Mode 2 is related to the longitudinal displacements of the deck where the middle point of the deck is regarded as an inflection point and has negligible vertical displacement. The third mode is like the first mode except that the piers lateral movement is in opposite directions. Mode 4 is mainly related to the vertical deflection of the middle span where the deck midpoint shows the largest camber. Mode 5 is like mode 4 except that the midpoint acts as an inflection point and its right- and left-side points move vertically in opposite directions. In mode 6, the middle span moves in lateral direction and at the same time, the deck rotates around its longitudinal axis due to torsion. The proposed control devices act in longitudinal direction and can have a major contribution to reduce dynamic responses due to the mode shapes with remarkable relative deflections in longitudinal direction.

2.3 Verification of the model

The OpenSees model is verified based on the available SAP2000 model provided by the designer company. The first three mode periods of the structure in OpenSees are 3.03, 2.97, and 2.37 s, respectively. The corresponding values in SAP2000 are 2.91, 2.82, and 2.39 s. The dynamic displacement response of OpenSees model is verified in Figs. 5(a) and 5(b). The displacements are recorded for the middle point of the deck in longitudinal direction.

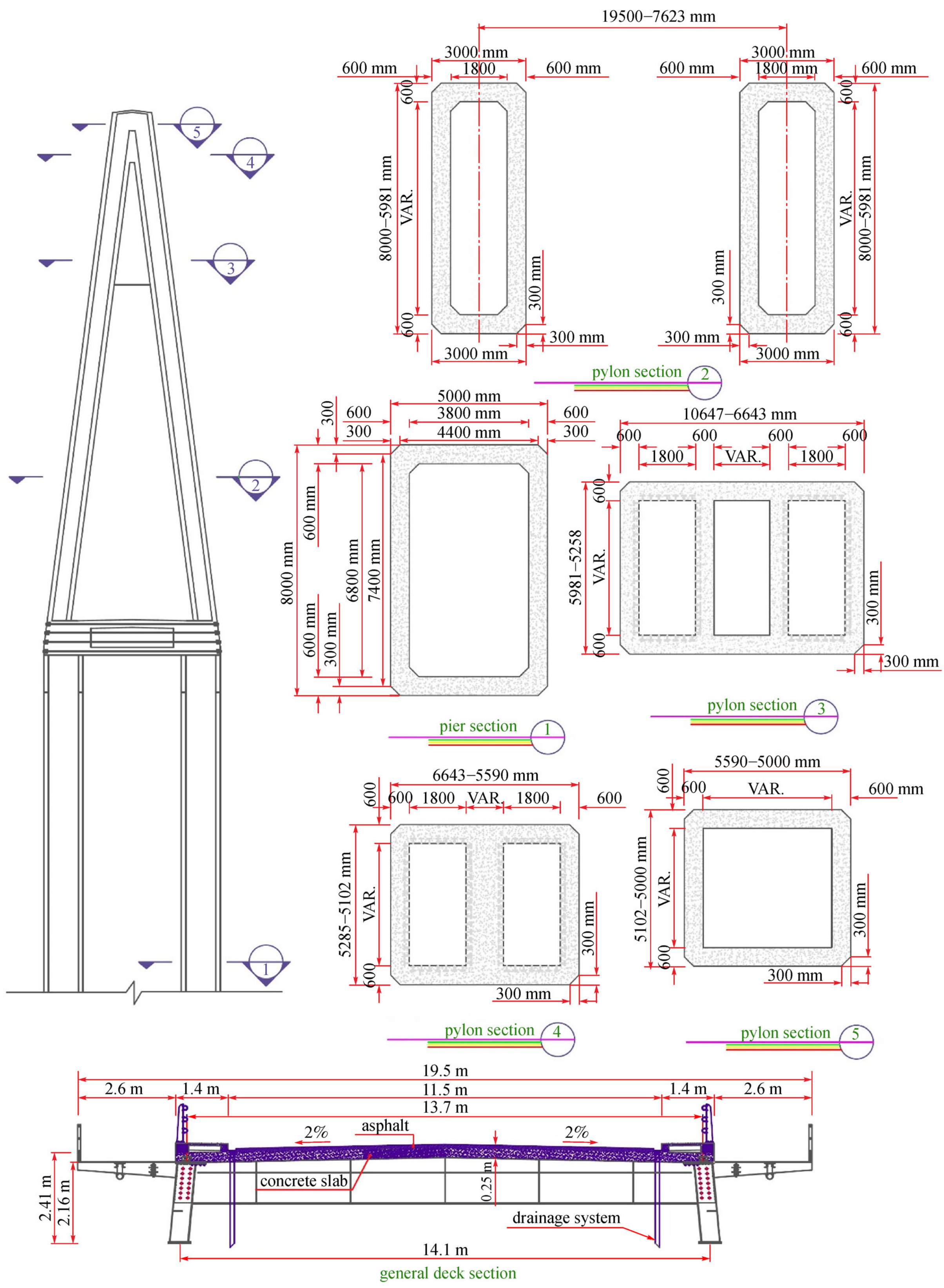

Fig. 2 Pier, pylon, and deck sections of the Lali Bridge.

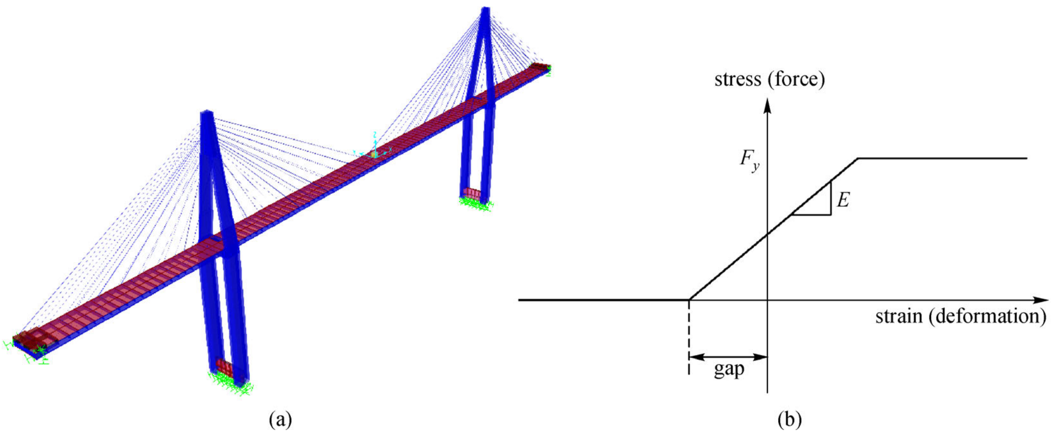

Fig. 3 Finite element model of the Lali Bridge: (a) overall view of the SAP2000 model; (b) mechanical behavior of tension-only material used for cables in OpenSees model.

Table 1 General characteristics of the finite element model of the bridge

parameter	element	value
yielding strength of steel	deck beams	360 MPa (ST52)
elastic modulus of steel	deck beams	2.1E5 MPa
yielding strength of steel	cables	1000 MPa
elastic modulus of steel	cables	1.95E5 MPa
compressive strength of concrete	deck slabs	45 MPa
compressive strength of concrete	piers	40 MPa
yielding strength of steel reinforcement	piers	400 MPa (S400)

Table 2 Parameters used for simulating the MR dampers

parameter	value
α_a	1.0872×10^5 N/cm
α_b	4.9616×10^5 N/(cm·V)
C_{0a}	4.40 N·s/cm
C_{0b}	44.0 N·s/(cm·V)
A_m	1.2
n	1
β	3 cm^{-1}
γ	3 cm^{-1}
η	50 s^{-1}

To achieve an even more precise verification, the obtained results for vertical displacements of the deck due to cable pre-stress forces and in the absence of other types of loads in the two models are compared in Fig. 5(c).

According to the period values, time history displacement responses, and the vertical displacements of the deck due to cable pre-stress forces, the OpenSees model is well-qualified to simulate the real behavior of the bridge. It is noteworthy that the slight discrepancies between the two models are the results of differences in the way that the two software packages simulate the nonlinear behavior of the structure. In OpenSees, nonlinear elements are modeled using fiber sections, while in SAP2000 plastic hinges are employed to simulate the nonlinear behavior. Moreover, unlike SAP2000, OpenSees can simulate the cracks in concrete material due to tension and accordingly consider the reduction of the element stiffness. Therefore, OpenSees provides more sophisticated facilities for simulating nonlinear behavior of structures. It is also worth bearing in mind that the responses of the two models in early seconds of the analysis, in which the majority of structural elements act in linear region, are significantly identical to each other (Figs. 5(a) and 5(b)). As the analysis continues, more structural elements enter the nonlinear region which results in appearing some differences between the results obtained from the two models.

3 Time history analyses

In this paper, nonlinear time history analyses are carried out using eight different ground excitations including four near field and four far field records. Four records are suggested by the International Association of Structural Control including El Centro1940, Hachinohe

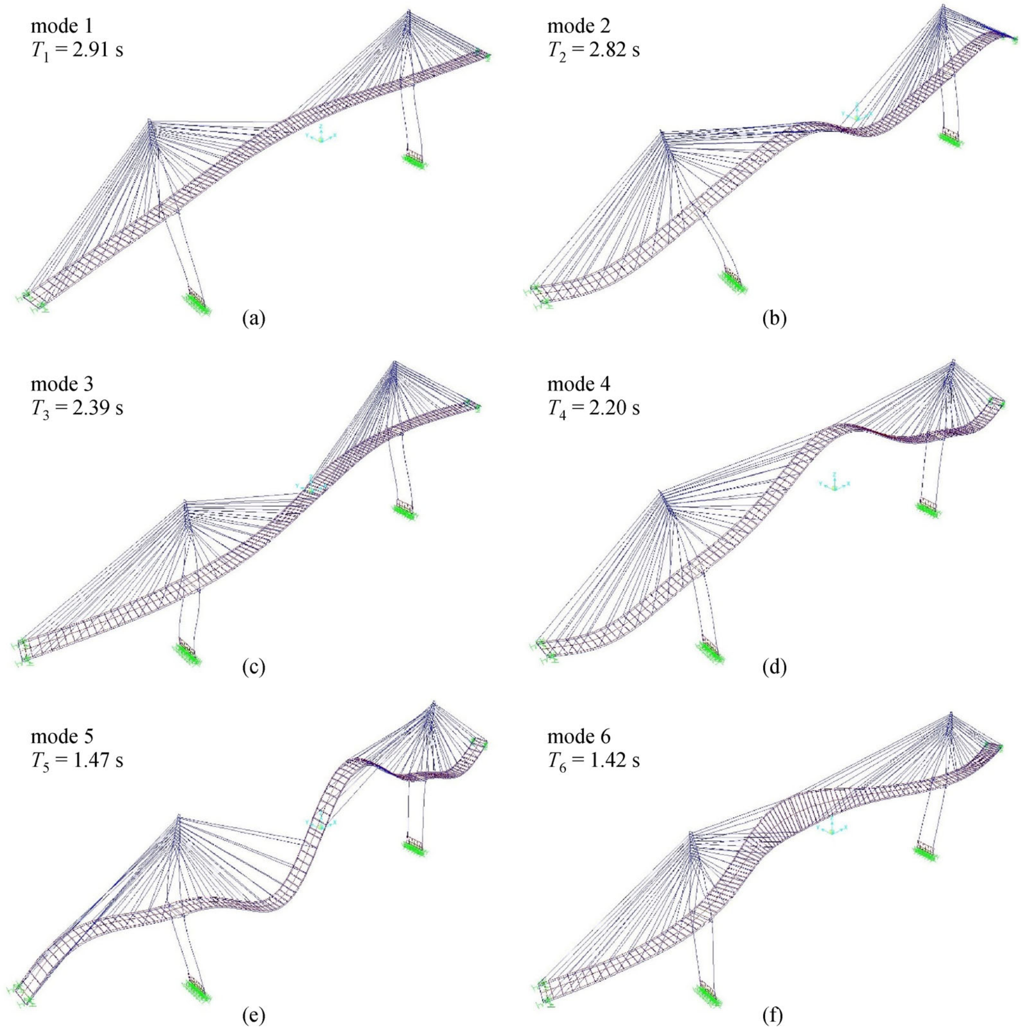

Fig. 4 The (a) first, (b) second, (c) third, (d) fourth, (e) fifth, and (f) sixth mode shapes of the Lali Bridge.

1968, Northridge 1994 and Kobe 1995 and four additional records are also considered to cover a wide range of excitation frequency content. The characteristics of the earthquake records are presented in Table 3. It should be noted that the traveling wave effect is not included in the time history analyses for simplicity.

The analyses are generally divided into three main categories. First, the aforementioned records are scaled based on the spectrums suggested by the Road, Housing, and Urban Development Research Center of the Ministry of Road and Urban Development of Iran for the seismic zone in which the Lali Bridge is located. The output data obtained from the time history analyses based on these scaled records are examined in order to determine the comparative efficiency of considered semi-active systems. Moreover, Incremental Dynamic Analysis (IDA) is employed to investigate the sensitivity of efficiency of proposed control systems to the PGA of the selected records. Finally, the effect of time lag is included in order to measure the consequential drop in efficiency of control systems subjected to scaled records.

To evaluate the efficiency of the control systems, 10 criteria denoted by J_1 to J_{10} are considered (Eq. (1)).

$$J_i = \frac{R_{i_c}}{R_{i_{uc}}}, \tag{1}$$

where ‘c’ and ‘uc’ stand for controlled and uncontrolled responses and R_i is defined as: the peak longitudinal displacement of the deck for $i = 1$; the peak longitudinal acceleration of the deck for $i = 2$; the peak base shear of piers for $i = 3$; the peak base moment of piers for $i = 4$; and the peak tensile stress of cables for $i = 5$. R_6 to R_{10} are similar to R_1 to R_5, respectively, except that instead of the peak response, the normed value of the corresponding response is used.

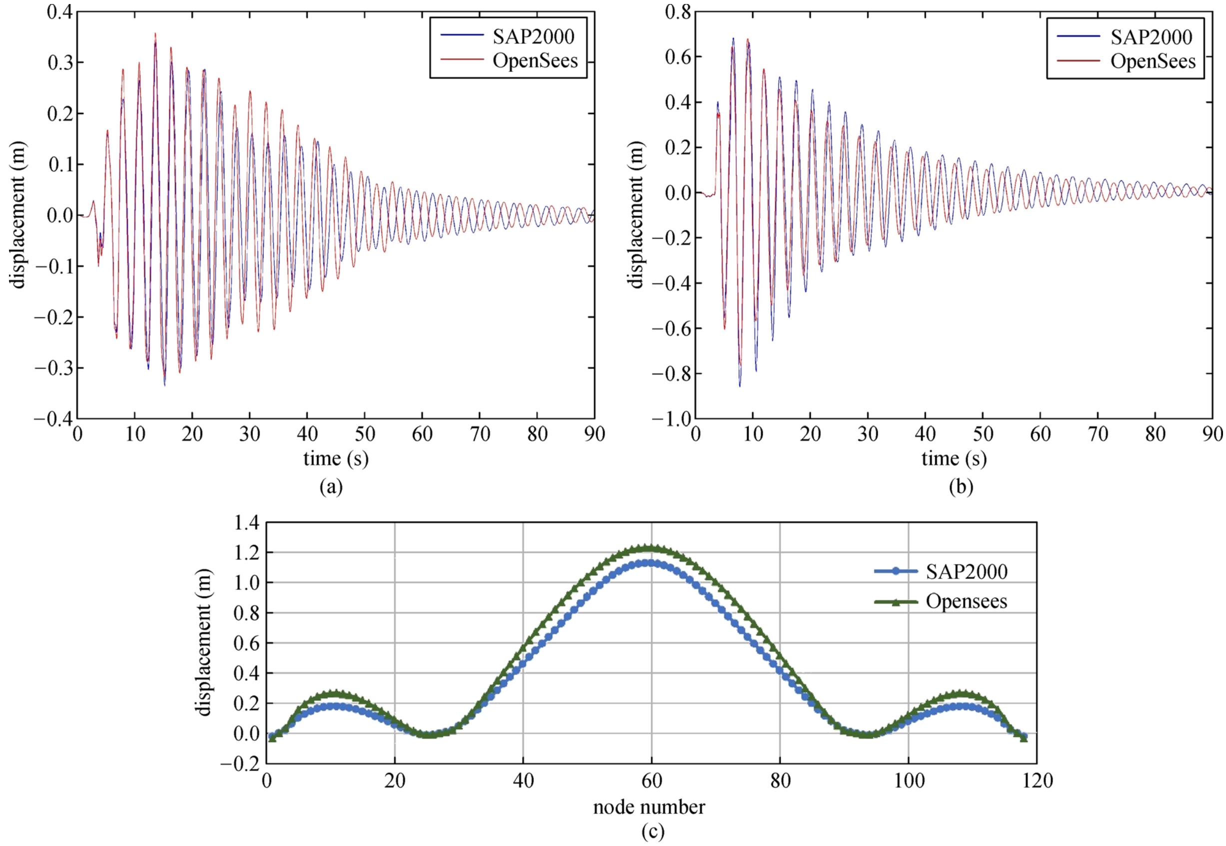

Fig. 5 Verification of the displacement response of the middle point of the deck subjected to (a) El Centro and (b) Northridge earthquake; (c) verification of the vertical displacements of the deck due to cable prestress forces.

Table 3 Characteristics of the ground motion records

record type	Earthquake	Station	PGA
near-field	Kobe, 1995	KJM	0.83g
	Northridge, 1994	Sylmar-Olive	0.84g
	Tabas, 1978	Tabas	0.85g
	Chi Chi, 1999	TCU065	0.83g
far-field	Imperial Valley, 1940	El Centro	0.35g
	Tokachi_Oki, 1968	Hachinohe	0.23g
	Tabas, 1978	Ferdows	0.11g
	Loma Prieta, 1989	Richmond City Hall	0.12g

4 MR damper model

To simulate the real behavior of a control system it is essential to use a comprehensive model for the control device. In this paper, a Bouc-Wen model, comparable to the one utilized by Ok et al. [30] is employed. As shown in Fig. 6(a), this model is comprised of a Bouc-Wen element in parallel with a dashpot. In this model, the control force produced by MR damper is obtained through the following Eqs [23]:

$$f = C_0\dot{x} + \alpha z, \tag{2}$$

$$\dot{z} = -\gamma|\dot{x}|z|\dot{z}|^{n-1} - \beta\dot{x}|z|^n + A_m\dot{x}, \tag{3}$$

where f is the control force, x is the displacement of the damper, and z is the evolutionary variable. γ, β, n, and A_m are presented in Tables 1 and 2. C_0 and α are determined based on the control voltage u through the following equations:

$$\alpha = \alpha(u) = \alpha_a + \alpha_b u, \tag{4}$$

$$C_0 = C_0(u) = C_{0a} + C_{0b}u, \tag{5}$$

where u is the applied control voltage and other parameters including α_a, α_b, C_{0a} , and C_{0b} are listed in Tables 1 and 2. To consider a time lag for applying the command voltage by the damper, the following equation is used

$$\dot{u} = -\eta(u-v), \tag{6}$$

where v is the command voltage applied to the control circuit and η is the time constant of the first-order filter. The hysteretic behavior of each MR damper is shown in Fig. 6(b).

In present study, the suggested control systems consist of a total of 24 MR dampers. Each damper can produce a maximum control force of 1000 kN. Each pier is connected to the deck using eight MR dampers, i.e., a total of 16 dampers are installed between the deck and pier 2 and 3. Similarly, four dampers are installed between the deck and bent 1, and four between the deck and bent 4. Figure 7 illustrates the schematic arrangement of MR dampers installed on the bridge. For describing the configuration of the measurement sensors, two types of points are demonstrated in Fig. 7. Each point of type 1 is the representative of one velocity sensor and one displacement sensor intended to measure the velocity and displacement of the deck in longitudinal direction, respectively. While, in each point of type 2 a pair of velocity and a pair of displacement sensors are installed to measure the velocity and displacement across the dampers.

5 Control algorithms

5.1 Sky-hook control algorithm

An on-off skyhook control algorithm is utilized in present study in which the input voltage of MR dampers is controlled by two values represented by high-state and low-state input voltages. The algorithm determines the input voltage of MR damper based on the following control laws:

$$\text{if } \dot{x}_1\dot{x}_{\text{rel}} \geqslant 0, \text{ then } v = 10, \tag{7}$$

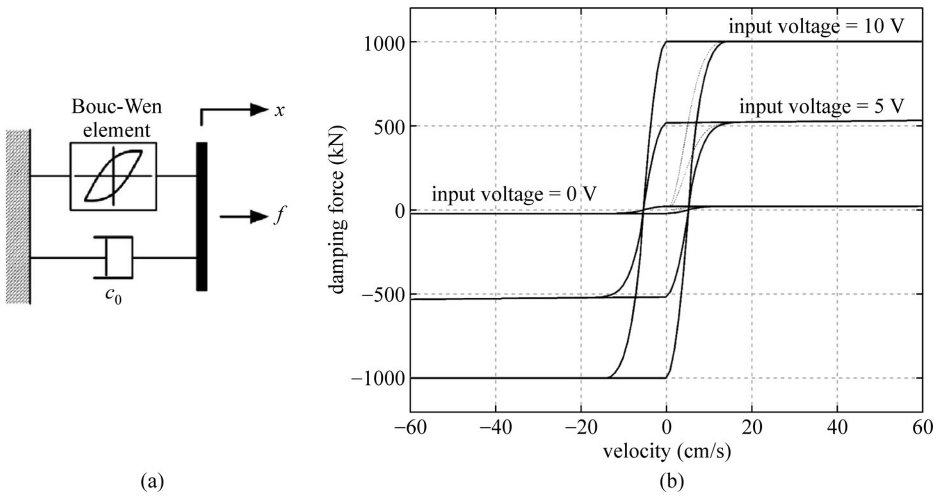

Fig. 6 (a) Schematic model of the MR damper; (b) hysteretic behavior of the MR damper for various values of input voltage.

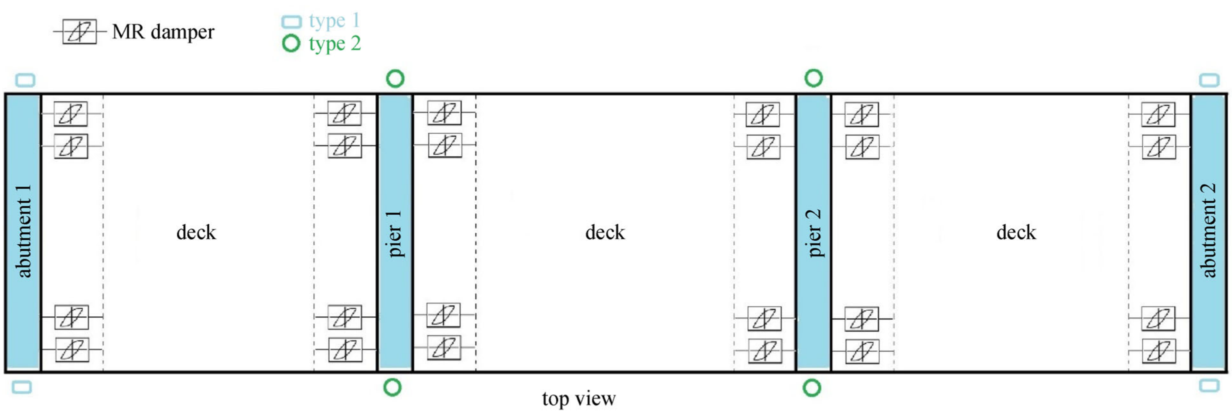

Fig. 7 Schematic arrangement of MR dampers and measurement sensors.

$$\text{if } \dot{x}_1\dot{x}_{\rm rel} < 0, \text{ then } v = 0, \quad (8)$$

where $\dot{x}_{\rm rel}$ is the relative velocity across the damper and $\dot{x}_1$ is the velocity of the joint between the damper and the deck.

5.2 FCA

Using Fuzzy Inference System (FIS) is a very powerful tool for dealing quickly and efficiently with imprecision and nonlinearity [35]. Hence, fuzzy control system is regarded as an efficient strategy to mitigate the vibration of complex structural systems with complicated nonlinear behavior.

Because of the advanced Fuzzy Logic Toolbox provided by MATLAB, this software is selected in order to apply semi-active algorithms in proposed control systems. The connection between OpenSees and MATLAB is devised using TCP IP. This service that is provided by TCL/TK programming language, creates a network connection through which servers and clients can contact to each other. In this study, the network connection is configured in a way that the dynamic response obtained from OpenSees model is transmitted to MATLAB in each step of time history analysis. Then the input voltage of MR dampers is calculated using Fuzzy Logic Toolbox. Afterwards, the damping forces are calculated based on the mechanical model of MR dampers and the obtained values are transmitted to OpenSees model. OpenSees exerts these forces to the structure and performs the next step of the analysis. This cycle continues until the last step of the analysis. This method enables us to benefit simultaneously from an accurate nonlinear dynamic simulation and a powerful mathematical tool for applying the algorithms.

To make the network connection, two servers and two clients are created in OpenSees using “socket” command. The servers and clients are denoted by Server 1, Server 2, Client 1, and Client 2. Client 1 and Client 2 are responsible for performing the codes written in Server 1 and Server 2, respectively. The code written in Server 1 includes the commands required for creating the structural model of the bridge, while Server 2 contains the commands related to exerting the control forces on the structure and performing one step of the analysis. Then, using a piece of code in MATLAB, Client 1 operates one time, i.e., OpenSees creates the structural model of the bridge. Afterwards, a loop containing the commands for operating Fuzzy Logic Toolbox and Client 2 is written. This loop iterates until all steps of analysis are done.

5.3 Configuration of the fuzzy algorithms

The responses of the structure recorded by the sensors are considered as the input variables for the fuzzy inference system and the MR damper command voltage is the output variable of the system. Each fuzzy inference system consists of fuzzification, rule-base, implication, and defuzzification module. For fuzzification of input variables, a total of 11 fuzzy sets are defined: NVL, NL, NM, NS, NVS, ZO, PVS, PS, PM, PL, and PVL. These sets are identified using the following abbreviations: N stands for negative, P for positive, S for small, M for medium, L for large, V for very, and ZO for zero. The corresponding membership functions of the defined sets for input variables are shown in Figs. 8(a), 8(b), and 8(c).

In the same way, for fuzzification of output variables, a total of six fuzzy sets are defined: VL, L, M, S, VS, and ZO. The corresponding membership functions of the defined sets are shown in Fig. 8(d).

A total of six different rule-bases denoted by RB1 to RB6 are utilized in fuzzy control systems named FIS1 to FIS6, respectively. Ok et al. [30] utilized a specific rule-base for fuzzy control of cable-stayed bridges which is adjusted to the current problem and is denoted by RB1. Symans and Kelly [28] proposed three rule-bases for semi-active fuzzy control of bridges. These rule-bases are adjusted to the current problem and are represented by RB2 to RB4. RB5 and RB6 are proposed based on the relative velocity across the damper as well as the absolute velocity of the end of damper connected to the deck. RB6 switches the command voltage between zero and 10 while RB5 can allocate any value between zero and 10 to the command voltage. Tables 4–9 presents the fuzzy rule tables used for RB1 to RB6. In these tables, the relative displacement and velocity across the MR damper are denoted by Disp and VelRel, respectively. The absolute velocity of the end of MR damper connected to the deck is denoted by Vel.

6 Results and commentary

The outputs of time history analyses based on the scaled records are considered to calculate the criteria for different controlled systems. The criteria are calculated separately for the eight excitation records and the average values are presented in Table 10.

According to Table 10, all control systems show higher performance in reducing the normed responses as opposed to peak responses. It is also observed that the control systems are not capable of remarkably reducing the cable tensions as the pre-stress forces are significantly large and the variations are relatively negligible. The sky-hook system efficiently reduces the displacements, but it has an undesirable influence on acceleration, base shear, base moment, and cable tension. FIS5 and FIS6 however, show satisfactory performance for all criteria.

Making the previous data more intuitive, the quantitative values are converted to qualitative variables including “P”, “F”, “G”, “VG”, and “E” describing the relative efficiency of control systems as “Poor”, “Fair”, “Good”, “Very Good”, and “Excellent”, respectively. For this purpose, the

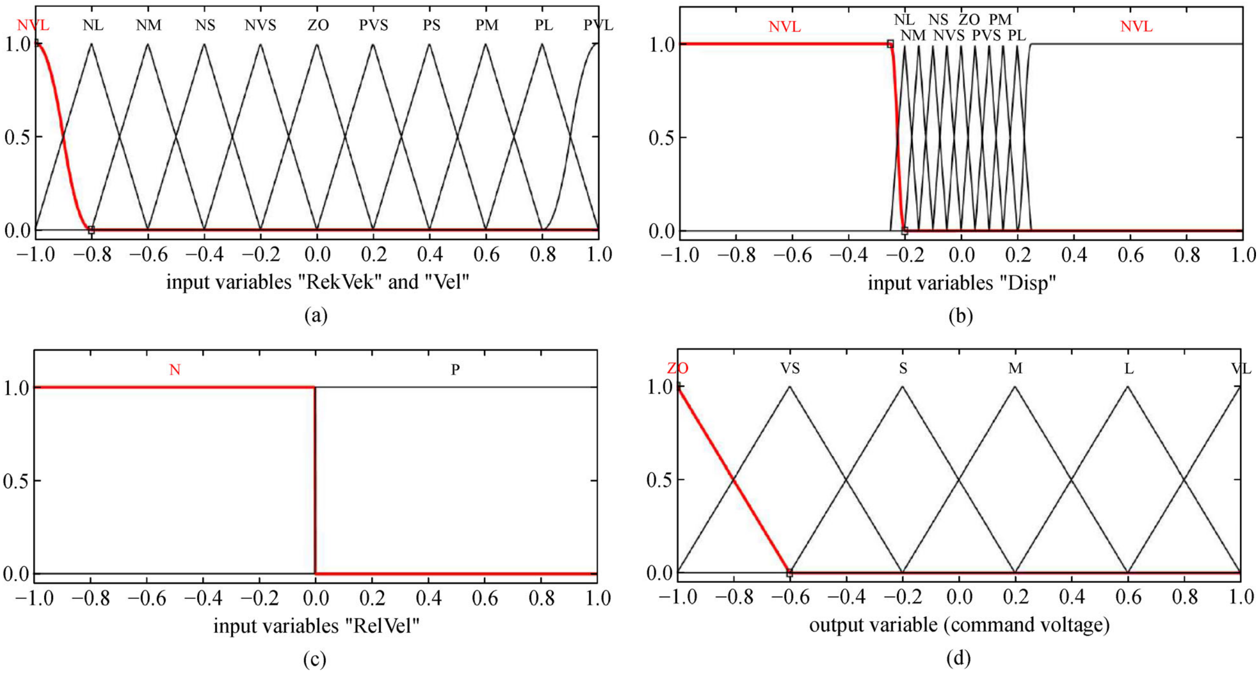

Fig. 8 Membership functions for (a) input variables used in rule base 1, 3, 4, and 5; (b) input variables used in rule base 2 and 3; (c) input variables used in rule base 2 and 6; (d) output variables (units are in SI).

Table 4 Fuzzy rule table for RB1

VelRel										
NVL	NL	NM	NS	NVS	ZO	PVS	PS	PM	PL	PVL
VL	L	M	S	VS	ZO	VS	S	M	L	VL

Table 5 Fuzzy rule table for RB2

		Disp										
		NVL	NL	NM	NS	NVS	ZO	PVS	PS	PM	PL	PVL
VelRel	P	ZO	ZO	ZO	ZO	ZO	VL	VL	VL	VL	VL	VL
	N	VL	VL	VL	VL	VL	VL	ZO	ZO	ZO	ZO	ZO

Table 6 Fuzzy rule table for RB3

		Disp										
		NVL	NL	NM	NS	NVS	ZO	PVS	PS	PM	PL	PVL
VelRel	PVL	L	VL	VL	VL	VL	VL	VL	VL	VL	VL	VL
	PL	M	L	VL	VL	VL	VL	VL	VL	VL	VL	VL
	PM	S	M	L	VL	VL	VL	VL	VL	VL	VL	VL
	PS	VS	S	M	L	VL	VL	VL	VL	VL	VL	VL
	PVS	ZO	VS	S	M	L	VL	VL	VL	VL	VL	VL
	ZO	VL	VL	VL	VL	VL	VL	VL	VL	VL	VL	VL
	NVS	VL	VL	VL	VL	VL	VL	L	M	S	VS	ZO
	NS	VL	VL	VL	VL	VL	VL	VL	L	M	S	VS
	NM	VL	VL	VL	VL	VL	VL	VL	VL	L	M	S
	NL	VL	VL	VL	VL	VL	VL	VL	VL	VL	L	M
	NVL	VL	VL	VL	VL	VL	VL	VL	VL	VL	VL	L

Table 7 Fuzzy rule table for RB4

VelRel										
NVL	NL	NM	NS	NVS	ZO	PVS	PS	PM	PL	PVL
ZO	VS	S	M	L	VL	L	M	S	VS	ZO

Table 8 Fuzzy rule table for RB5

		Vel										
		NVL	NL	NM	NS	NVS	ZO	PVS	PS	PM	PL	PVL
VelRel	PVL	ZO	ZO	ZO	ZO	ZO	ZO	VS	S	M	L	VL
	PL	ZO	ZO	ZO	ZO	ZO	VS	S	M	L	VL	VL
	PM	ZO	ZO	ZO	ZO	ZO	S	M	L	VL	VL	VL
	PS	ZO	ZO	ZO	ZO	ZO	M	L	VL	VL	VL	VL
	PVS	ZO	ZO	ZO	ZO	ZO	L	VL	VL	VL	VL	VL
	ZO	VL	VL	VL	VL	VL	VL	VL	VL	VL	VL	VL
	NVS	VL	VL	VL	VL	VL	L	ZO	ZO	ZO	ZO	ZO
	NS	VL	VL	VL	VL	L	M	ZO	ZO	ZO	ZO	ZO
	NM	VL	VL	VL	L	M	S	ZO	ZO	ZO	ZO	ZO
	NL	VL	VL	L	M	S	VS	ZO	ZO	ZO	ZO	ZO
	NVL	VL	L	M	S	VS	ZO	ZO	ZO	ZO	ZO	ZO

Table 9 Fuzzy rule tables for RB6

		Vel										
		NVL	NL	NM	NS	NVS	ZO	PVS	PS	PM	PL	PVL
VelRel	P	ZO	ZO	ZO	ZO	ZO	VL	VL	VL	VL	VL	VL
	N	VL	VL	VL	VL	VL	VL	ZO	ZO	ZO	ZO	ZO

Table 10 Average performance criteria for control systems subjected to scaled earthquake records

control system	J_1	J_2	J_3	J_4	J_5	J_6	J_7	J_8	J_9	J_{10}
FIS1	0.630	0.889	0.969	0.919	0.931	0.430	0.645	0.570	0.448	0.993
FIS2	0.739	1.072	1.057	1.166	0.992	0.538	0.779	0.897	0.714	0.999
FIS3	0.648	0.965	1.014	1.034	0.972	0.400	0.737	0.706	0.614	0.995
FIS4	0.698	0.981	1.002	1.065	0.967	0.506	0.749	0.734	0.576	0.995
FIS5	0.465	1.016	0.992	1.001	0.985	0.325	0.668	0.674	0.454	0.998
FIS6	0.433	1.011	0.998	1.006	1.000	0.290	0.726	0.734	0.495	0.999
sky-hook	0.420	1.048	1.020	1.028	1.016	0.233	0.956	0.906	0.751	0.999
passive	0.575	0.969	0.957	0.966	0.956	0.361	0.775	0.637	0.488	0.995

variation range of data in each column is divided into 5 equal intervals and the data in each interval are referred to as the above variables respectively. Table 11 presents the qualitative efficiency of the control systems subjected to scaled earthquake records.

To make a general judgment about the best suited algorithm for vibration control of the Lali Bridge, the relative importance of each criterion should be specified. It can be determined according to the effect of each criterion on improvement of structural behavior of the bridge. Moreover, consequential economic impacts related to each criterion can also be another important factor. However, determining the relative importance of each criterion is considered as an engineering decision-making procedure which can be done by the designer. This process enables the designer to adjust the control system in order to achieve desired structural performance requirements. In the present study, a typical evaluation of relative importance of each criterion is considered. According to Table 12 each criterion is allocated a number between 0 and 10 which is proportional to its importance. Accordingly, the overall priority of control systems is assessed in the last column of Table 11.

The results of IDA analyses are considered in order to judge about the sensitivity of control systems to the PGA of excitation records. Figure 9 shows the variations of J_1 versus PGA for El Centro earthquake using various control algorithms. Similar graphs for other earthquakes confirm that the semi-active control systems can reduce the maximum value of displacement of the deck by 80% for relatively small values of PGA and more than 40% for large values.

To assess the sensitivity of control systems to the PGA of excitation records, the averaged absolute values of slope in these graphs are considered. The average slope for each control system is calculated by considering all evaluation criteria and excitation records and the results are presented in Table 13. The quantitative data are interpreted qualitatively in order to determine the relative sensitivity of efficiency of control systems to the PGA of excitation records. The average slope of graphs is also calculated for each criterion in order to evaluate the average variation of efficiency of control systems for improving each criterion due to an increase in PGA (Table 14). A positive slope in Table 14 shows an increase in performance criteria and therefore a decrease in efficiency of control systems, and vice versa. The results show that FIS1 exhibits a remarkably stable behavior against PGA variations and is regarded as a very reliable control system for a wide range of PGA.

Including the effect of a 0.1 s time lag in fuzzy control systems, the performance criteria are calculated and compared with corresponding values without time lag. Table 15 shows the average values of relative errors caused by the time lag. According to this table, FIS1 is the most stable control system in presence of the time lag. On the other hand, the efficiency of FIS6 significantly decreases due to time lag. It can be also inferred that the tensile stress of cables is not sensitive to time lag, whereas the deck acceleration exhibits a remarkable sensitivity.

For stay cables, it is not adequate to merely examine the peak and the normed values of tensile stress. Another

Table 11 Overall qualitative evaluation of efficiency of control systems

	qualitative efficiency										overall ranking
FIS1	F	E	E	E	E	F	E	E	E	E	5
FIS2	P	P	P	P	F	P	G	P	P	P	8
FIS3	F	G	G	G	G	G	VG	G	G	VG	6
FIS4	P	G	G	G	G	P	VG	G	G	VG	7
FIS5	E	F	VG	VG	F	VG	E	VG	E	F	2
FIS6	E	F	G	VG	P	E	VG	G	E	P	1
sky-hook	E	P	F	G	P	E	P	P	P	P	3
passive	G	G	E	E	VG	G	G	E	E	VG	4

Table 12 Relative importance of each criterion considered for the overall evaluation

criterion	J_1	J_2	J_3	J_4	J_5	J_6	J_7	J_8	J_9	J_{10}
relative importance	10.0	0.2	2.0	2.0	2.0	10.0	4.0	2.0	2.0	0.2

Table 13 Evaluation of sensitivity of control systems to PGA

control system	average slope	sensitivity of efficiency to PGA
FIS1	0.128	very stable
FIS2	0.338	very sensitive
FIS3	0.319	very sensitive
FIS4	0.341	very sensitive
FIS5	0.256	sensitive
FIS6	0.325	very sensitive
sky-hook	0.346	very sensitive
passive	0.284	sensitive

Table 14 Evaluation of sensitivity of performance criteria to PGA

criterion	average slope	variation of control systems efficiency due to increase in PGA
J_1	0.403	very significant decrease
J_2	–0.440	very significant increase
J_3	0.121	moderate decrease
J_4	0.435	very significant decrease
J_5	0.070	no meaningful change
J_6	0.215	significant decrease
J_7	–0.114	moderate increase
J_8	0.302	very significant decrease
J_9	0.353	very significant decrease
J_{10}	–0.002	no meaningful change

Table 15 The average percentage of relative errors due to a 0.1 sec time lag

control system	relative error (%)										
	J_1	J_2	J_3	J_4	J_5	J_6	J_7	J_8	J_9	J_{10}	average
FIS1	3.77	7.02	2.23	6.99	0.16	11.82	150.98	7.30	8.81	0.02	19.91
FIS2	18.91	148.06	1.42	−2.11	0.10	43.10	485.77	24.32	43.63	0.11	76.33
FIS3	11.24	167.74	1.09	−0.76	0.45	36.32	642.47	7.32	10.55	0.04	87.65
FIS4	9.30	83.98	2.75	−1.32	−1.56	35.74	321.68	6.36	9.68	−0.01	46.66
FIS5	25.63	142.16	7.17	1.86	3.99	39.54	598.95	6.96	11.05	0.03	83.74
FIS6	26.63	148.53	12.86	0.23	0.92	46.46	656.11	5.17	8.68	0.05	90.57
average	15.91	116.25	4.59	0.82	0.68	35.50	475.99	9.57	15.40	0.04	

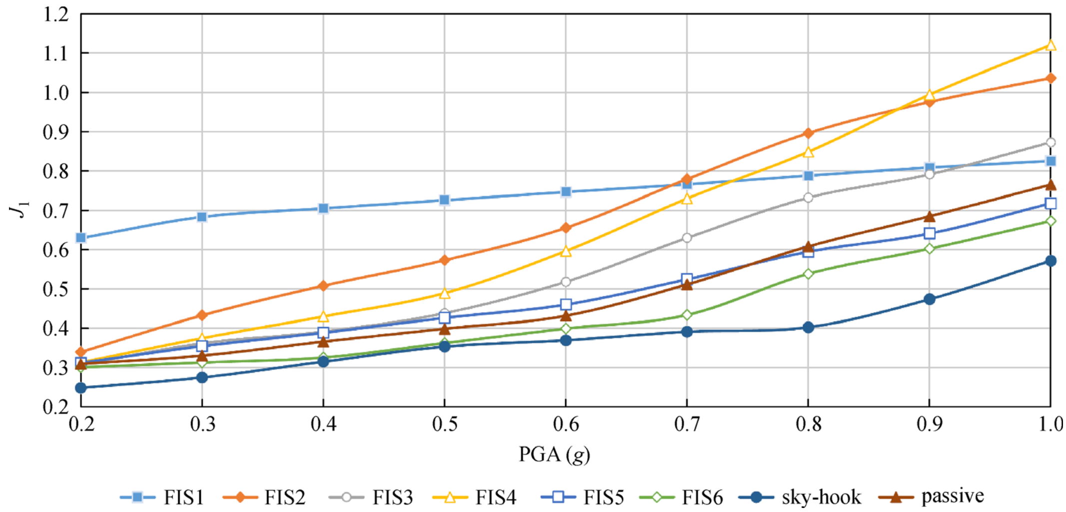

Fig. 9 Variation of J_1 vs. PGA for El Centro earthquake.

essential issue that should be considered is the unseating of cables. For examining the probability of unseating and failure of the cables, an acceptable interval for tension of each stay cable is assumed. Accordingly, a lower bound of $0.2T_{fi}$ and an upper bound of $1.0T_{fi}$ are selected for the acceptable region, where T_{fi} is the yielding tension of the cable. The acceptable and actual regions related to different control systems and different excitation records are drawn and thoroughly examined. The results show that the most efficient system to reduce the failure and unseating probability is FIS1 (Fig. 10(a)). Conversely, the probability of failure and unseating of cables for FIS6 is higher than the other systems including passive-on, sky-hook, and other fuzzy systems. The likelihood of failure and unseating of cables for FIS6 subjected to Northridge record is shown in Fig. 10(b).

7 Conclusions

For utilizing a semi-active fuzzy control system in order to reduce the earthquake-induced vibrations of the Lali Cable-Stayed Bridge, a comprehensive nonlinear 3D model was built in OpenSees. The validity of the model was verified based on the model provided by the designer company in SAP2000. A connection between OpenSees and MATLAB was devised. This connection led to a convenient method for applying semi-active control algorithms to nonlinear complex structures like cable-stayed bridges. A general layout for installing MR dampers and sensors was considered. A Bouc-Wen model was utilized to simulate MR dampers mechanical behavior. A total of six fuzzy rule-bases were employed to control the vibration of the Lali Bridge subjected to several seismic excitation records. Two rule-bases were proposed by the authors and the other four ones were obtained by adopting the rule-bases suggested by other researchers. The effectiveness of FCAs was compared to each other and also to sky-hook and passive-on control systems. Furthermore, the sensitivity of efficiency of control systems to the PGA of excitation records was thoroughly investigated. At

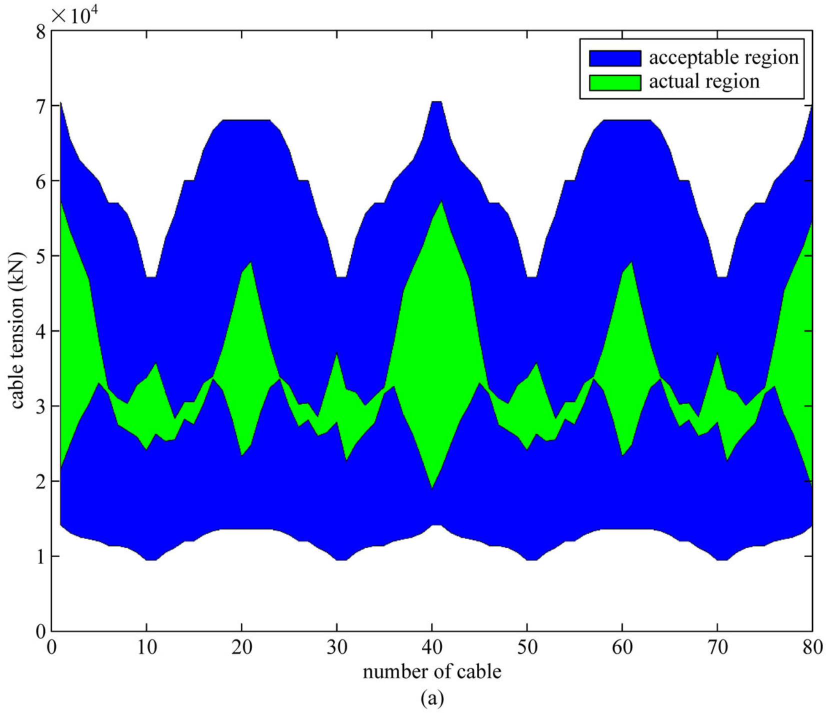

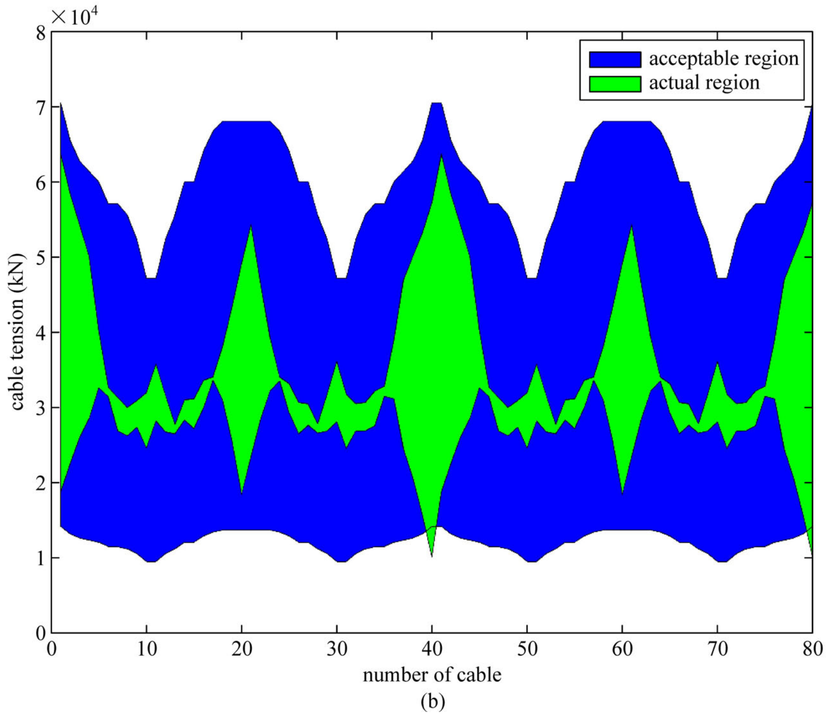

Fig. 10 Evaluation of failure and unseating of cables for (a) FIS1, (b) FIS6 subjected to Northridge record.

last, the effect of time lag was included in order to estimate the consequential drop in efficiency of control systems.

The results showed that the semi-active control systems proposed in this study can reduce the maximum value of displacement of the deck by 80% for relatively small values of PGA and more than 40% for large values. It was also observed that fuzzy control can reduce the maximum acceleration of the deck by up to 30%. A design procedure was also described, and the qualitative results were prepared in a way that can be regarded as a general guide for design of semi-active fuzzy control systems for vibration control of cable-stayed bridges.

Acknowledgements Invaluable support of Bolandpayeh Company for providing the model of Lali Bridge in SAP2000 is gratefully appreciated. The assistance of Mrs. N. Zangeneh and Mr. M. Kamali-Zarch in preparing technical information about Lali Bridge is acknowledged. The kind cooperation of Mr. R. Zamanian for applying TCP IP network connection is also appreciated.

References

1. George H W. Influence of deck material on response of cable-stayed bridges to live loads. Journal of Bridge Engineering, 1999, 4(2): 136–142
2. Mehrabi A B. In-service evaluation of cable-stayed bridges, overview of available methods and findings. Journal of Bridge Engineering, 2006, 11(6): 716–724
3. Hasan M, Khalil E, Attia W, Turkey A. Influence of deck longitudinal prestressing on cable-stayed bridges. Structural Engineering International, 2015, 25(3): 292–299
4. Caicedo J M, Dyke S J, Moon S J, Bergman L A, Turan G, Hague S. Phase II benchmark control problem for seismic response of cable-stayed bridges. Structural Control and Health Monitoring, 2003, 10(3–4): 137–168
5. Nariman N A. A novel structural modification to eliminate the early coupling between bending and torsional mode shapes in a cable-stayed bridge. Frontiers of Structural and Civil Engineering, 2017, 11(2): 131–142
6. Abdel-Ghaffar A M. Cable-stayed bridges under seismic action. In: Proceedings of the Seminar Cable-Stayed Bridges: Recent Devel-Opment and Their Future. Yokohama, 1991
7. Housner G, Bergman L A, Caughey T K, Chassiakos A G, Claus R O, Masri S F, Skelton R E, Soong T T, Spencer B F, Yao J T. Structural control: Past, present, and future. Journal of Engineering Mechanics, 1997, 123(9): 897–971
8. Symans M D, Constantinou M C. Semi-active control systems for seismic protection of structures: A state-of-the-art review. Engineering Structures, 1999, 21(6): 469–487
9. Fujino Y. Vibration, control and monitoring of long-span bridges—Recent research, developments and practice in Japan. Journal of Constructional Steel Research, 2002, 58(1): 71–97
10. Spencer B F Jr, Nagarajaiah S. State of the art of structural control. Journal of Structural Engineering, 2003, 129(7): 845–856
11. Javadinasab Hormozabad S, Ramezani M, Ghorbani-Tanha A K. Seismic behavior and vibration control of Lali Cable-Stayed Bridge using TMD. In: Proceedings of the 4th International Conference on Bridge (4IBC2015). Tehran, 2015
12. Spencer B F Jr, Dyke S J, Sain M K, Carlson J. Phenomenological model for magnetorheological dampers. Journal of Engineering Mechanics, 1997, 123(3): 230–238
13. He W L, Agrawal A K, Mahmoud K. Control of seismically excited cable-stayed bridge using resetting semiactive stiffness dampers. Journal of Bridge Engineering, 2001, 6(6): 376–384
14. Bitaraf M, Ozbulut O E, Hurlebaus S, Barroso L. Application of semi-active control strategies for seismic protection of buildings with MR dampers. Engineering Structures, 2010, 32(10): 3040–3047
15. El-Khoury O, Kim C, Shafieezadeh A, Hur J E, Heo G H. Experimental study of the semi-active control of a nonlinear two-span bridge using stochastic optimal polynomial control. Smart Materials and Structures, 2015, 24(6): 065011
16. Miah M S, Chatzi E N, Dertimanis V K, Weber F. Real-time experimental validation of a novel semi-active control scheme for vibration mitigation. Structural Control and Health Monitoring, 2017, 24(3): e1878
17. Javadinasab Hormozabad S, Zahrai S M. Innovative adaptive viscous damper to improve seismic control of structures. Journal of Vibration and Control, 2019, 25(12): 1833–1851
18. Dyke S J, Caicedo J M, Turan G, Bergman L A, Hague S. Phase I benchmark control problem for seismic response of cable-stayed bridges. Journal of Structural Engineering, 2003, 129(7): 857–872
19. Iemura H, Pradono M H. Application of pseudo-negative stiffness control to the benchmark cable-stayed bridge. Structural Control and Health Monitoring, 2003, 10(3–4): 187–203
20. Yang J N, Lin S, Jabbari F. H2-based control strategies for civil engineering structures. Structural Control and Health Monitoring, 2003, 10(3–4): 205–230
21. Agrawal A K, Yang J N, He W L. Applications of some semiactive control systems to benchmark cable-stayed bridge. Journal of Structural Engineering, 2003, 129(7): 884–894
22. Dyke S J, Spencer B F Jr, Sain M K, Carlson J D. Modeling and control of magnetorheological dampers for seismic response reduction. Smart Materials and Structures, 1996, 5(5): 565–575
23. Jansen L M, Dyke S J. Semiactive control strategies for MR dampers: Comparative study. Journal of Engineering Mechanics, 2000, 126(8): 795–803
24. Yi F, Dyke S J, Caicedo J M, Carlson J D. Experimental verification of multi-input seismic control strategies for smart dampers. Journal of Engineering Mechanics, 2001, 127(11): 1152–1164
25. Ramallo J C, Johnson E A, Spencer B F Jr. “Smart” base isolation systems. Journal of Engineering Mechanics, 2002, 128(10): 1088–1099
26. Xu L H, Li Z X. Semi-active multi-step predictive control of structures using MR dampers. Earthquake Engineering & Structural Dynamics, 2008, 37(12): 1435–1448
27. Jung H J, Spencer B F Jr, Lee I W. Control of seismically excited cable-stayed bridge employing magnetorheological fluid dampers. Journal of Structural Engineering, 2003, 129(7): 873–883
28. Symans M D, Kelly S W. Fuzzy logic control of bridge structures using intelligent semi-active seismic isolation systems. Earthquake Engineering & Structural Dynamics, 1999, 28(1): 37–60
29. Park K S, Koh H M, Ok S Y, Seo C W. Fuzzy supervisory control of earthquake-excited cable-stayed bridges. Engineering Structures, 2005, 27(7): 1086–1100
30. Ok S Y, Kim D S, Park K S, Koh H M. Semi-active fuzzy control of cable-stayed bridges using magneto-rheological dampers. Engineering Structures, 2007, 29(5): 776–788
31. Yoshioka H, Ramallo J C, Spencer B F Jr. “Smart” base isolation strategies employing magnetorheological dampers. Journal of Engineering Mechanics, 2002, 128(5): 540–551
32. Johnson E A, Baker G A, Spencer B F Jr, Fujino Y. Semiactive damping of stay cables. Journal of Engineering Mechanics, 2007,

133(1): 1–11

33. Salari S, Javadinasab Hormozabad S, Ghorbani-Tanha A K, Rahimian M. Innovative mobile TMD system for semi-active vibration control of inclined sagged cables. KSCE Journal of Civil Engineering, 2019, 23(2): 641–653
34. Ghahramani A. Static and dynamic analysis of Lali bridge basin and caisson foundation. In: Proceedings of the 8th International Congress on Civil Engineering. Shiraz, 2009
35. MATLAB. Fuzzy Logic Toolbox^{TM} User's Guide. Natick, MA: The Math Works, Inc., 2011